INTERNATIONAL JOURNAL OF ROBUST AND NONLINEAR CONTROL
Int. J. Robust Nonlinear Control 2009; **19**:1959–1971
Published online 21 April 2009 in Wiley InterScience (www.interscience.wiley.com). DOI: 10.1002/rnc.1424

Analytical formulation to compute QFT bounds: The envelope method

Juan José Martín-Romero[1,*,†], Montserrat Gil-Martínez[2] and Mario García-Sanz[3]

[1]*Department of Electrical and Electronic Engineering, IES Manuel Bartolomé Cossío, 26200 Haro, Spain*
[2]*Department of Electrical Engineering, University of La Rioja, 26004 Logroño, Spain*
[3]*Department of Automatic Control and Computer Science, Public University of Navarra, 31006 Pamplona, Spain*

SUMMARY

This paper describes an analytical formulation to compute quantitative feedback theory (QFT) bounds in one-degree-of-freedom feedback control problems. The new approach is based on envelope curves and shows that a QFT control specification can be expressed as a family of circumferences. Then, the controller bound is defined by the envelope curve of this family and can be obtained as an analytical function. This offers the possibility of studying the QFT bounds in an analytical way with several useful properties. Gridding methods are avoided, resulting in a lower computational effort procedure. The new formulation improves the accuracy of previous methods and allows the designer to calculate multivalued bounds. Copyright © 2009 John Wiley & Sons, Ltd.

Received 28 November 2007; Revised 15 April 2008; Accepted 10 November 2008

KEY WORDS: quantitative feedback theory (QFT); uncertain systems; robust control

1. INTRODUCTION

Quantitative feedback theory (QFT) [1, 2] has proven to be an efficient and practical engineering methodology in a large number of cases [3–5]. In the first QFT Symposium (1992) Prof. Horowitz said: 'There is room in QFT for highly diverse talents: the non-mathematical practical engineer with physical insight and inventive talent, the skilled mathematician interested in existence theorems and abstract generalizations, up to the stubborn, even plodding researcher who by hard dedicated work acquires deep understanding of this subject'. He added: 'QFT is as yet in its infancy, pointing to vast, available problem areas'. Much progress has been made and many difficulties have been overcome in the last 15 years. However, as Horowitz insisted in the fifth QFT Symposium [6] that analysis is still true today. In fact, basic (but not simple) problems such as template or bound calculation have not been completely solved yet. This paper focuses on the bound computation problem, looking for a new formulation that obtains analytical QFT bounds for one-degree-of-freedom (1 DoF) control cases.

QFT bounds are the limits (maximum and/or minimum) of the open-loop nominal transfer function $L_o(j\omega) = P_o(j\omega)G(j\omega)$ at each frequency that guarantees to meet the required closed-loop control specifications for all the plants in the uncertainty set. QFT specifications for minimum phase systems

*Correspondence to: Juan José Martín-Romero, Department of Electrical and Electronic Engineering, IES Manuel Bartolomé Cossío, 26200 Haro, Spain.
†E-mail: juanjo@cossio.net

Contract/grant sponsor: Ministerio de Ciencia y Tecnología; contract/grant number: CICYT DPI'2006-15522-C02-01
Contract/grant sponsor: La Rioja Government; contract/grant number: ANGI 2004/13

are formulated as inequalities of certain magnitude transfer functions for the desired closed-loop frequency response. Using these specifications and taking the templates into account (model plus uncertainty), the QFT bounds are computed; one for each robust control specification and frequency. A ω_i-template is the set of all possible values of the uncertain plant at frequency ω_i. Only the boundary of this ω_i-template is necessary for the controller design. This contour of the template at ω_i will be labelled as $\mathscr{T}_{\omega_i}$ [7, 8].

Originally, QFT bounds were calculated by using manual graphical manipulations of plant templates on the Nichols chart. Searching for a solution to this tedious procedure, several researches developed some algorithms for automatic bound computation. Early bound generation algorithms used geometrical and/or search-based CAD techniques [9–13]. Afterwards, more efficient numerical algorithms based on quadratic inequalities were proposed [14–18]. These algorithms established a formal process that mapped plant uncertainty and feedback specifications into the bound expressions through quadratic inequalities. They form the basis of the bound computation in the well-known QFT Toolbox [19]. The Qsyn [20], another CAD solution, improves bound calculation using algorithms based on the *cross section* concept [21–23]. Algorithms based on quadratic inequalities are only able to find out two values of the QFT bound (maximum and minimum values) at one phase $\phi\in[-2\pi, 0]$, whereas those based on cross section calculate all possible values (multivalued bounds). Some examples of multivalued bounds are shown for the robust tracking specification in [22, 23]. At the end of this work another example of multivalued bound is shown for the robust control effort specification. Other works that improve the efficiency and accuracy of the algorithms are in [24–26]. However, all of them present trade-offs between accuracy and computation time: they are based on computational nested loops for discrete sets according to uncertainty, frequency and the bound phase.

This paper extends [27, 28] and describes an analytical formulation that uses envelope curves to compute the QFT bounds for 1 DoF control systems. It avoids former gridding methods thus improving accuracy and reducing computational effort.

In Section 2 the envelope method is expounded. Section 3 particularizes the solution for robust noise rejection and robust stability problems. Section 4 solves the bound computation for control specifications based on the sensitivity function (i.e. the robust disturbance rejection at the plant output). The problem of robust disturbance rejection at the plant input is considered in Section 5. Section 6 makes the same with the control effort bound and Section 7 shows some remarks. Two examples for different robust control specifications illustrate the methodology in Section 8. Finally, the conclusions are presented in Section 9.

2. THE ENVELOPE METHOD

Let us consider the classical 1 DoF control diagram shown in Figure 1, where the plant $\mathscr{P}(s)$ has uncertainty, the reference input $r(t)$ is constant and the remaining blocks are known.

A general single-input–single-output QFT control specification can be expressed as:

$$\left|\frac{A(\mathrm{j}\omega_i,\varphi)+B(\mathrm{j}\omega_i,\varphi)\mathscr{G}_{\omega_i}}{1+C(\mathrm{j}\omega_i,\varphi)\mathscr{G}_{\omega_i}}\right|\leqslant\gamma(\omega_i)$$
$$\forall\omega_i\in[\omega_{\min},\omega_{\max}] \tag{1}$$

Note that $\gamma(\omega_i)$ is the upper limit of the control specification magnitude at the frequency ω_i and $A=ae^{\mathrm{j}\vartheta_a}=A_r+\mathrm{j}A_i$, $B=be^{\mathrm{j}\vartheta_b}=B_r+\mathrm{j}B_i$ and $C=ce^{\mathrm{j}\vartheta_c}=C_r+\mathrm{j}C_i$ are complex functions. They depend on the plant template values, which are given by $\mathscr{T}_{\omega_i}(\varphi)$.[‡] $\mathscr{G}_{\omega_i}=ge^{\mathrm{j}\phi}=g_{\mathrm{re}}+\mathrm{j}g_{\mathrm{im}}$ is the controller bound[§] for the $\gamma(\omega_i)$ control specification. As long as each control specification provides a $\mathscr{G}_{\omega_i}$, $\mathscr{G}^{(1)}_{\omega_i}$ is the bound controller for the specification $|\mathscr{P}G/(1+\mathscr{P}G)|\leqslant\gamma_1$, $\mathscr{G}^{(2)}_{\omega_i}$ for $|1/(1+\mathscr{P}G)|\leqslant\gamma_2$, $\mathscr{G}^{(3)}_{\omega_i}$ for $|\mathscr{P}/(1+\mathscr{P}G)|\leqslant\gamma_3$ and $\mathscr{G}^{(4)}_{\omega_i}$ for $|G/(1+\mathscr{P}G)|\leqslant\gamma_4$. Then, without loosing generality, it is assumed that $H(s)=1$. γ_1, γ_2, γ_3 and

[‡] In general, $\mathscr{T}_{\omega_i}(\varphi)$ is supposed to be an analytical continuous and differentiable function of $\varphi\in[0, 2\pi]$ that defines the template contour at ω_i [7, 8]. Nevertheless, the methodology is also valid for discrete φ arrays (discrete templates).

[§] The QFT bound to perform the loopshaping is $\mathscr{B}_{\omega_i}=P_o\mathscr{G}_{\omega_i}$, where P_o is the nominal plant.

DOI: 10.1002/rnc

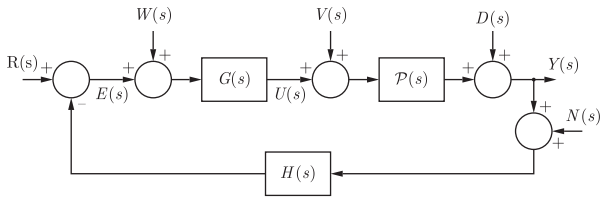

Figure 1. Classical control structure.

γ_4 are magnitude frequency models of the desired closed-loop performance or stability specifications in a classical feedback control structure (G: controller, $\mathscr{P}$: plant).

Equation (1) can be rewritten using imaginary and real parts as

$$\left|\frac{A_r+\mathrm{j}A_i+(B_r+\mathrm{j}B_i)(g_{\mathrm{re}}+\mathrm{j}g_{\mathrm{im}})}{1+(C_r+\mathrm{j}C_i)(g_{\mathrm{re}}+\mathrm{j}g_{\mathrm{im}})}\right|\leqslant\gamma \tag{2}$$

to obtain a quadratic inequality:

$$\begin{aligned}&((C_r^2+C_i^2)\gamma^2-(B_r^2+B_i^2))(g_{\mathrm{re}}^2+g_{\mathrm{im}}^2)\\&+2(\gamma^2C_r-A_rB_r-A_iB_i)g_{\mathrm{re}}\\&-2(\gamma^2C_i+A_iB_r-A_rB_i)g_{\mathrm{im}}\\&+\gamma^2-A_r^2-A_i^2\geqslant 0\end{aligned} \tag{3}$$

A_r, A_i, B_r, B_i, C_r, C_i can be a function of $\mathscr{T}_{\omega_i}$ and depend on a parameter φ used to track the plant template contour. Taking (3) as an equation (mathematical expression equals zero), a circumference family (one circumference for each φ value) is obtained. The structure of this family is

$$(g_{\mathrm{re}}-g_{\mathrm{rc}})^2+(g_{\mathrm{im}}-g_{\mathrm{ic}})^2=r^2 \tag{4}$$

where the center (real and imaginary parts) is defined by

$$\begin{aligned}g_{\mathrm{rc}}(\varphi)&=\frac{-\gamma^2C_r+A_rB_r+A_iB_i}{(C_r^2+C_i^2)\gamma^2-B_r^2-B_i^2}\\g_{\mathrm{ic}}(\varphi)&=\frac{\gamma^2C_i+A_iB_r-A_rB_i}{(C_r^2+C_i^2)\gamma^2-B_r^2-B_i^2}\end{aligned} \tag{5}$$

and the radius is

$$r(\varphi)=\frac{\gamma\sqrt{(z_1-z_2)}}{(C_r^2+C_i^2)\gamma^2-B_r^2-B_i^2} \tag{6}$$

being

$$\begin{aligned}z_1&=(A_r^2+A_i^2)(C_r^2+C_i^2)+B_r^2+B_i^2\\z_2&=2(A_rB_r+A_iB_i)C_r-2(A_iB_r-A_rB_i)C_i\end{aligned}$$

If the plant does not have uncertainty, expression (4) is a circumference that delimitates the area where the controller can be defined in the Re–Im plane; that is, the controller bound $\mathscr{G}_{\omega_i}$. On the other hand, if there is uncertainty, the controller bound $\mathscr{G}_{\omega_i}$ is the contour of the circumference family (the envelope curve [29]). Therefore, the bound problem is reduced to computing the envelope curve of the family (4). The circumference family can be written in a parametric form as

$$\begin{aligned}&g_{\mathrm{rc}}(\varphi)+r(\varphi)\cos\theta\\&g_{\mathrm{ic}}(\varphi)+r(\varphi)\sin\theta\end{aligned} \tag{7}$$

where $\theta\in[0,2\pi]$. Each point of the envelope curve is obtained by computing the intersection of two infinitesimally close circumferences. Then, an infinitesimally close circumference to (7) is

$$\begin{aligned}&g_{\mathrm{rc}}(\varphi+\Delta\varphi)+r(\varphi+\Delta\varphi)\cos\theta\\&g_{\mathrm{ic}}(\varphi+\Delta\varphi)+r(\varphi+\Delta\varphi)\sin\theta\end{aligned} \tag{8}$$

being $\Delta\varphi$ an infinitesimal variation of φ. The intersection between (7) and (8) yields

$$\begin{aligned}g_{\mathrm{rc}}(\varphi)+r(\varphi)\cos\theta_1&=g_{\mathrm{rc}}(\varphi+\Delta\varphi)\\&\quad+r(\varphi+\Delta\varphi)\cos(\theta_2)\\g_{\mathrm{ic}}(\varphi)+r(\varphi)\sin\theta_1&=g_{\mathrm{ic}}(\varphi+\Delta\varphi)\\&\quad+r(\varphi+\Delta\varphi)\sin(\theta_2)\end{aligned} \tag{9}$$

As long as φ and $\varphi+\Delta\varphi$ are infinitesimally close, θ_1 and θ_2 are infinitesimally close too. Therefore, making

DOI: 10.1002/rnc

$\theta_1=\theta$ and $\theta_2=\theta+\Delta\theta$, it is found that

$$\begin{aligned} g_{\mathrm{rc}}(\varphi)+r(\varphi)\cos\theta &= g_{\mathrm{rc}}(\varphi+\Delta\varphi) \\ &\quad +r(\varphi+\Delta\varphi)\cos(\theta+\Delta\theta) \\ g_{\mathrm{ic}}(\varphi)+r(\varphi)\sin\theta &= g_{\mathrm{ic}}(\varphi+\Delta\varphi) \\ &\quad +r(\varphi+\Delta\varphi)\sin(\theta+\Delta\theta) \end{aligned} \tag{10}$$

If it is supposed that $f(x+\Delta x)=f(x)+\Delta f(x)=f(x)+f'(x)\Delta x$, expression (10) can be reduced to

$$\begin{aligned} g'_{\mathrm{rc}}(\varphi)\Delta\varphi+r'(\varphi)\cos\theta\Delta\varphi &= r(\varphi)\sin\theta\Delta\theta \\ &\quad +r'(\varphi)\sin\theta\Delta\varphi\Delta\theta \\ g'_{\mathrm{ic}}(\varphi)\Delta\varphi+r'(\varphi)\sin\theta\Delta\varphi &= -r(\varphi)\cos\theta\Delta\theta \\ &\quad +r'(\varphi)\cos\theta\Delta\varphi\Delta\theta \end{aligned} \tag{11}$$

where

$$g'_{\mathrm{rc}}(\varphi)=\frac{\mathrm{d}g_{\mathrm{rc}}(\varphi)}{\mathrm{d}\varphi}, \quad g'_{\mathrm{ic}}(\varphi)=\frac{\mathrm{d}g_{\mathrm{ic}}(\varphi)}{\mathrm{d}\varphi} \quad \text{and}$$

$$r'(\varphi)=\frac{\mathrm{d}r(\varphi)}{\mathrm{d}\varphi}$$

Obtaining $\Delta\theta$ from every equation and making equal both expressions:

$$\begin{aligned} &\frac{g'_{\mathrm{rc}}(\varphi)+r'(\varphi)\cos(\theta)}{r(\varphi)\sin\theta+r'(\varphi)\sin\theta\Delta\varphi} \\ &\quad =\frac{g'_{\mathrm{ic}}(\varphi)+r'(\varphi)\sin(\theta)}{r(\varphi)\cos\theta+r'(\varphi)\cos\theta\Delta\varphi} \end{aligned} \tag{12}$$

The limit of (12) when $\Delta\varphi\to 0$ provides

$$g'_{\mathrm{rc}}(\varphi)\cos\theta+g'_{\mathrm{ic}}(\varphi)\sin\theta+r'(\varphi)=0 \tag{13}$$

By solving (13), it is obtained

$$\theta_{1,2}(\varphi)=\arctan\left(\frac{-g'_{\mathrm{ic}}(\varphi)r'(\varphi)\mp g'_{\mathrm{rc}}(\varphi)\sqrt{g'_{\mathrm{ic}}(\varphi)^2+g'_{\mathrm{rc}}(\varphi)^2-r'(\varphi)^2}}{-g'_{\mathrm{rc}}(\varphi)r'(\varphi)\pm g'_{\mathrm{ic}}(\varphi)\sqrt{g'_{\mathrm{ic}}(\varphi)^2+g'_{\mathrm{rc}}(\varphi)^2-r'(\varphi)^2}}\right) \tag{14}$$

where

$$g'_{\mathrm{rc}}(\varphi)=\frac{\mathrm{d}g_{\mathrm{rc}}(\varphi)}{\mathrm{d}\varphi}, \quad g'_{\mathrm{ic}}(\varphi)=\frac{\mathrm{d}g_{\mathrm{ic}}(\varphi)}{\mathrm{d}\varphi} \quad \text{and}$$

$$r'(\varphi)=\frac{\mathrm{d}r(\varphi)}{\mathrm{d}\varphi}$$

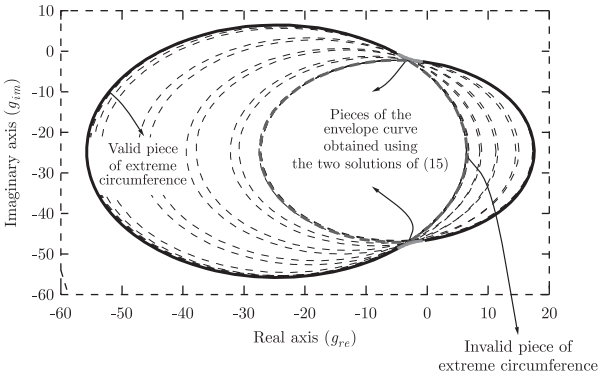

Figure 2. Controller bound from an open template. Note that the curves shown are circumferences, but the picture is on a scale that make them seem ellipses.

If the template contour $\mathscr{T}_{\omega_i}$ is closed, the curve of the centers $(g_{\mathrm{rc}}, g_{\mathrm{ic}})$ is closed too. The two solutions in (14) provide the outer envelope curve and the inner one. The controller bound is defined by the inner envelope curve if the radius $r(\varphi)$ of some circumference of the family is negative and it is defined by the outer one in the other case.[¶] Then, the controller bound $\mathscr{G}_{\omega_i}$ can be expressed as a function of φ:

$$\mathscr{G}_{\omega_i}(\varphi)=\begin{cases} g_{\mathrm{rc}}(\varphi)+r(\varphi)\cos(\theta(\varphi)) \\ g_{\mathrm{ic}}(\varphi)+r(\varphi)\sin(\theta(\varphi)) \end{cases} \tag{15}$$

If $\mathscr{T}_{\omega_i}$ is an open curve, the two solutions and a portion of the extreme circumferences are necessary to calculate the envelope curve. Figure 2 shows a family of circumferences (dashed lines) obtained from an open template. Solid black lines are defined by the extreme circumferences and solid gray lines are given by the two solutions of (14).

The previous calculation of the controller bound assumes that the intersection of two infinitesimally close circumferences exists. However, if the square

[¶]This can be proved by taking into account the inequality (3) and the structure of the circumference family, which is defined by expressions (4)–(6).

DOI: 10.1002/rnc

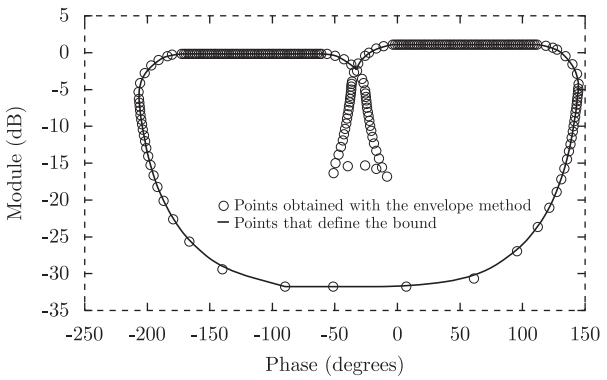

Figure 3. Robust stability bound $\mathscr{B}_{\omega_i}^{(1)} = P_o \mathscr{G}_{\omega_i}^{(1)}$ obtained by the envelope method using a template with a strong concavity.

root of (14) results in a complex number, some circumferences of the family are inner (or outer) to their infinitesimally close ones and there is no intersection. This situation arises when

$$g'_{\mathrm{ic}}(\varphi)^2 + g'_{\mathrm{rc}}(\varphi)^2 - r'(\varphi)^2 < 0 \tag{16}$$

Then, the $\mathscr{T}_{\omega_i}(\varphi)$ points that keep (16) do not generate bound points and should be eliminated. According to this a new template contour $\mathscr{T}_{\omega_i}^{\varepsilon}$, labelled *equivalent template*, should be obtained. The equivalent template is the set of all the points of the template contour $\mathscr{T}_{\omega_i}$ that generates all the points of the bound. In Section 4, it is explained how to use $\mathscr{T}_{\omega_i}^{\varepsilon}$ to calculate the controller bound.

Another particular case arises when the template has a deep concavity. Then, the bound obtained using (15) could not be a Jordan curve (a simple and closed curve) and some pieces of this would not be relevant for the controller design. Figure 3 illustrates this problem at $s = \mathrm{j}\omega = \mathrm{j}1$ for the uncertain plant

$$\mathscr{P} = \frac{\mathrm{e}^{-Ts}}{s^2 + 0.04s + \omega_n^2}$$

shown in [30], where $T \in [0, 2]$ and $\omega_n \in [0.7, 1.2]$, and a control specification $|\mathscr{P}G/(1+\mathscr{P}G)| < 1.82$. The envelope method provides the curve marked with circles; the effective QFT bound is the solid black line. A complementary analysis of this problem can be found in [31].

Finally, if the template is non-connected a controller bound must be found for every piece of it. After that, the intersection of valid surfaces must be computed to find the final controller bound. An example is shown in Section 4.

3. ROBUST STABILITY AND NOISE REJECTION BOUNDS

Robust stability and robust noise attenuation specifications are defined as

$$\left| \frac{\mathscr{P}(\mathrm{j}\omega_i)\mathscr{G}_{\omega_i}}{1 + \mathscr{P}(\mathrm{j}\omega_i)\mathscr{G}_{\omega_i}} \right| \leqslant \gamma_1(\omega_i) \tag{17}$$

where $\gamma_1(\omega_i) = \gamma_1$ is a real number[‖] for a fixed frequency ω_i. Comparing with (1): $A = 0$ and $B = C = P(\mathrm{j}\omega_i) = \mathscr{T}_{\omega_i} = p_{\mathrm{re}} + \mathrm{j}p_{\mathrm{im}}$. Then, (17) can be written as

$$\left| \frac{(g_{\mathrm{re}} + \mathrm{j}g_{\mathrm{im}})(p_{\mathrm{re}}(\varphi) + \mathrm{j}p_{\mathrm{im}}(\varphi))}{1 + (g_{\mathrm{re}} + \mathrm{j}g_{\mathrm{im}})(p_{\mathrm{re}}(\varphi) + \mathrm{j}p_{\mathrm{im}}(\varphi))} \right| \leqslant \gamma_1 \tag{18}$$

The circumference family is

$$\begin{aligned} &\frac{-p_{\mathrm{re}}(\varphi)\dfrac{\gamma_1^2}{\gamma_1^2 - 1}}{p_{\mathrm{re}}(\varphi)^2 + p_{\mathrm{im}}(\varphi)^2} + \frac{\dfrac{\gamma_1}{\gamma_1^2 - 1}}{\sqrt{p_{\mathrm{re}}(\varphi)^2 + p_{\mathrm{im}}(\varphi)^2}} \cos(\theta) \\ &\frac{p_{\mathrm{im}}(\varphi)\dfrac{\gamma_1^2}{\gamma_1^2 - 1}}{p_{\mathrm{re}}(\varphi)^2 + p_{\mathrm{im}}(\varphi)^2} + \frac{\dfrac{\gamma_1}{\gamma_1^2 - 1}}{\sqrt{p_{\mathrm{re}}(\varphi)^2 + p_{\mathrm{im}}(\varphi)^2}} \sin(\theta) \end{aligned} \tag{19}$$

The solutions in (14) are valid if (16) is not kept. The worst case appears when the template comes from an uncertain gain because

$$r(\varphi) = \frac{\dfrac{\gamma_1}{\gamma_1^2 - 1}}{\sqrt{p_{\mathrm{re}}(\varphi)^2 + p_{\mathrm{im}}(\varphi)^2}}$$

and its maximum variation $r'(\varphi)$ appears with a maximum change of the module $\sqrt{p_{\mathrm{re}}(\varphi)^2 + p_{\mathrm{im}}(\varphi)^2}$.

[‖]This number indicates the desired gain and phase margins $MG \geqslant 1 + 1/\gamma_1$ and $MF \geqslant 180° - 2\arccos 1/2\gamma_1$ or the desired noise reduction at ω_i.

DOI: 10.1002/rnc

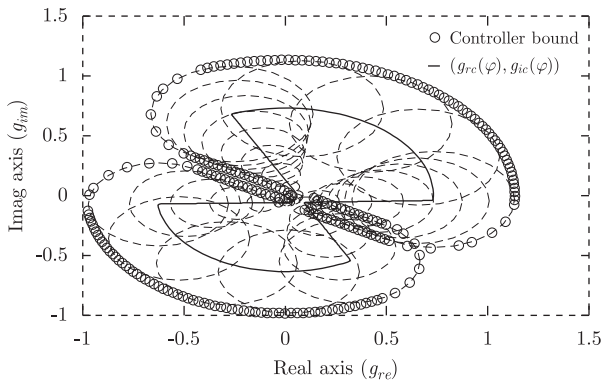

Figure 4. Controller bound $(g_{\mathrm{re}}(\varphi), g_{\mathrm{im}}(\varphi))$ and its circumference family.

Thus, the most unfavorable template** is

$$\mathscr{T}_{\omega i}(\varphi)=\begin{cases} m_1\varphi \\ m_2\varphi \end{cases} \tag{20}$$

where m_1 and m_2 are constants. Obtaining $g_{\mathrm{rc}}(\varphi)$, $g_{\mathrm{ic}}(\varphi)$ and $r(\varphi)$, and substituting them in (16), the condition of intersection existence between two infinitesimally close circumference is

$$\frac{\gamma_1^2}{(\gamma_1^2-1)(m_1^2+m_2^2)\varphi^4}>0 \tag{21}$$

If $\gamma_1>1$, the earlier expression is always true and the controller bound is obtained substituting (14) in (19). Figure 4 shows the bound controller on the Re–Im plane for the plant

$$\mathscr{P}=\frac{\mathrm{e}^{-Ts}}{s^2+0.04s+\omega_n^2}$$

and the case described in Section 2 (see Figure 3), where the outer envelope curve has been selected. The circumference family and the $(g_{\mathrm{rc}}(\varphi), g_{\mathrm{ic}}(\varphi))$ curve are also shown.

**On the other hand, the most favorable case arises if the template comes from an uncertain delay in the dynamic plant. Then, the radius variation $r'(\varphi)$ is zero because the module is a real number.

For feedback control specifications with $\gamma_1<1$, a procedure such as the one described in Section 4 must be used.

4. ROBUST SENSITIVITY BOUNDS

The robust sensitivity specification imposes an upper limit in the magnitude so that

$$\left|\frac{1}{1+\mathscr{P}(\mathrm{j}\omega_i)\mathscr{G}_{\omega_i}}\right|<\gamma_2 \tag{22}$$

According to (3), with $A=1$, $B=0$ and $C=P(\mathrm{j}\omega_i)=\mathscr{T}_{\omega_i}=p_{\mathrm{re}}+\mathrm{j}p_{\mathrm{im}}$, (22) can be written as

$$\begin{aligned}(p_{\mathrm{im}}(\varphi)^2+p_{\mathrm{re}}(\varphi)^2)(g_{\mathrm{im}}^2+g_{\mathrm{re}}^2)+2(p_{\mathrm{re}}(\varphi)g_{\mathrm{re}}\\ -p_{\mathrm{im}}(\varphi)g_{\mathrm{im}})+1-\frac{1}{\gamma_2^2}\geqslant 0\end{aligned} \tag{23}$$

The family of circumferences appears when (23) equals 0:

$$\begin{aligned}&-\frac{p_{\mathrm{re}}(\varphi)}{p_{\mathrm{re}}(\varphi)^2+p_{\mathrm{im}}(\varphi)^2}+\frac{\gamma_2^{-1}}{\sqrt{p_{\mathrm{re}}(\varphi)^2+p_{\mathrm{im}}(\varphi)^2}}\cos(\theta)\\ &\frac{p_{\mathrm{im}}(\varphi)}{p_{\mathrm{re}}(\varphi)^2+p_{\mathrm{im}}(\varphi)^2}+\frac{\gamma_2^{-1}}{\sqrt{p_{\mathrm{re}}(\varphi)^2+p_{\mathrm{im}}(\varphi)^2}}\sin(\theta)\end{aligned} \tag{24}$$

The intersection between two infinitesimally close circumferences must exist to accomplish the substitution of the θ parameter in (14). The less favorable case occurs when the radius variation reaches the maximum, that is, if the template comes from an uncertain gain: $\mathscr{T}_{\omega_i}=(p_{\mathrm{re}}(\varphi), p_{\mathrm{im}}(\varphi))=(m_1\varphi, m_2\varphi)$, where m_1, m_2 are constants and φ is the uncertain parameter. Under these conditions, (16) is evaluated obtaining,

$$\frac{\dfrac{\gamma_2^2-1}{\gamma_2^2}}{\varphi^4(m_1^2+m_2^2)}<0 \tag{25}$$

Inequality (25) is not achieved if γ_2 is greater than 1. Then, the envelope method can be applied by

DOI: 10.1002/rnc

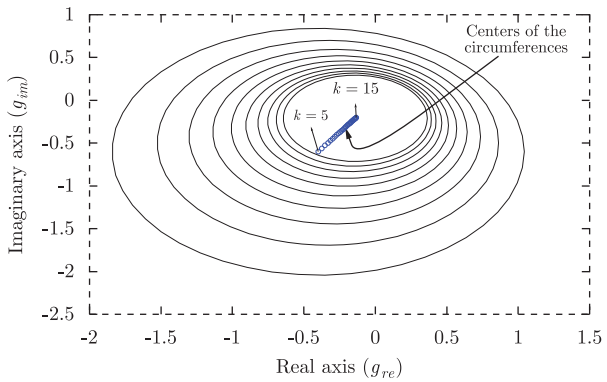

Figure 5. Circumference family without intersections.

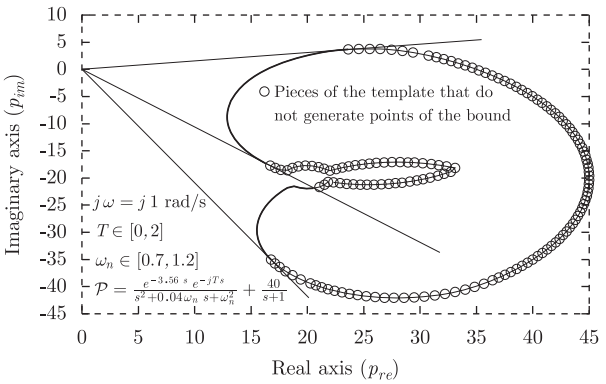

Figure 6. Example of valid pieces of the template and non valid ones to calculate $\mathcal{G}^{(2)}_{\omega_i}$.

substituting (14) into (19). According to (25), if $\gamma_2 < 1$ the square roots of (14) are complex. Imagine a plant $\mathcal{P} = k/(s+2)$ with $k \in [5, 15]$, $\omega = 3$ rad/s and $\gamma_2 = 0.5$, the circumference family would be the one shown in Figure 5. A similar behaviour is obtained for the control specification in (17) with $\gamma_1 < 1$.

This proves that in each set of template points with the same phase, only the lowest gain point of this set generates a point of the controller bound; the other points of this set can be eliminated. Figure 6 illustrates this with an example; the circled points of the template have no influence on the controller bound. What is more, some of the rest of the points could not generate bound points if some circumferences were within others. It depends on the value of γ_2 and is simple to determine by computation.

Those template points that generate bound points define the equivalent template $\mathcal{T}^{\varepsilon}_{\omega_i}$. Figure 7 shows the equivalent template for two different γ_2 values.

If the equivalent template is open and differentiable in its extremes, the envelope curve can be obtained without using pieces of the extreme circumferences.†† Defining $\mathcal{T}^{\varepsilon}_{\omega_i}$ as

$$\mathcal{T}^{\varepsilon}_{\omega_i} = \mathcal{T}_{\omega_i}(\varphi) \quad \text{with } \varphi \in [\varphi_1, \varphi_2] \tag{26}$$

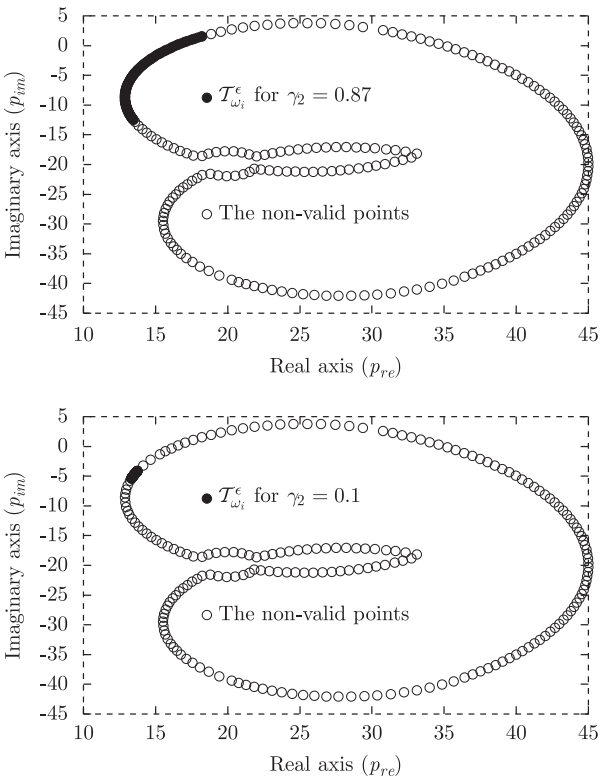

Figure 7. Equivalent template $\mathcal{T}^{\varepsilon}_{\omega_i}$ for two γ_2 values.

††In Section 2 it is explained how to calculate a controller bound from an open template that is non-differentiable in its extremes.

DOI: 10.1002/rnc

and being $\mathscr{T}_{\omega_i}(\varphi)$ continuous and differentiable in $\varphi \in [\varphi_1-\varepsilon_\varphi, \varphi_2+\varepsilon_\varphi]$, where ε_φ is infinitesimal, for the angles

$$\theta_1 = \arctan\left(\frac{-g'_{\mathrm{ic}}(\varphi_1)r'(\varphi_1)-g'_{\mathrm{rc}}(\varphi_1)\sqrt{g'_{\mathrm{ic}}(\varphi_1)^2+g'_{\mathrm{rc}}(\varphi_1)^2-r'(\varphi_1)^2}}{-g'_{\mathrm{rc}}(\varphi_1)r'(\varphi_1)+g'_{\mathrm{ic}}(\varphi_1)\sqrt{g'_{\mathrm{ic}}(\varphi_1)^2+g'_{\mathrm{rc}}(\varphi_1)^2-r'(\varphi_1)^2}}\right)$$
$$\theta_2 = \arctan\left(\frac{-g'_{\mathrm{ic}}(\varphi_2)r'(\varphi_2)+g'_{\mathrm{rc}}(\varphi_2)\sqrt{g'_{\mathrm{ic}}(\varphi_2)^2+g'_{\mathrm{rc}}(\varphi_2)^2-r'(\varphi_2)^2}}{-g'_{\mathrm{rc}}(\varphi_2)r'(\varphi_2)-g'_{\mathrm{ic}}(\varphi_2)\sqrt{g'_{\mathrm{ic}}(\varphi_2)^2+g'_{\mathrm{rc}}(\varphi_2)^2-r'(\varphi_2)^2}}\right) \quad (27)$$

it is obtained,

$$\begin{aligned} g_{\mathrm{rc}}(\varphi_1)+r(\varphi_1)\cos(\theta_1) &= g_{\mathrm{rc}}(\varphi_2)+r(\varphi_2)\cos(\theta_2) \\ g_{\mathrm{ic}}(\varphi_1)+r(\varphi_1)\sin(\theta_1) &= g_{\mathrm{ic}}(\varphi_2)+r(\varphi_2)\sin(\theta_2) \end{aligned} \quad (28)$$

This means that the controller bound can be completely computed by evaluating (15) with the points of $\mathscr{T}^{\varepsilon}_{\omega_i}$. However, there are templates that are not continuous and differentiable in $[\varphi_1-\varepsilon_\varphi, \varphi_2+\varepsilon_\varphi]$. In these cases, it is necessary to take some points of the extreme[‡‡] circumferences as explained in Section 2. Figure 8 shows an example where $\mathscr{T}^{\varepsilon}_{\omega_i}$ is defined by two pieces that are not differentiable in their extremes.

The two pieces of $\mathscr{T}^{\varepsilon}_{\omega_i}$ define two 'sub-bounds' of the controller, $\mathscr{G}'_{\omega_i}$ and $\mathscr{G}''_{\omega_i}$. The controller bound $\mathscr{G}^2_{\omega_i}$ is the intersection[§§] of both.

5. ROBUST DISTURBANCE REJECTION AT THE PLANT INPUT BOUNDS

The control specification for robust disturbance rejection at plant input is $|\mathscr{P}/(1+\mathscr{P}G)| \leqslant \gamma_3$. Then, $B(\mathrm{j}\omega)=0$ and $A=C=\mathscr{T}_{\omega i}(\varphi)=p_{\mathrm{re}}(\varphi)+\mathrm{j}p_{\mathrm{im}}(\varphi)$ in (1). By using (5) and (6) and substituting in (7), the circumference family is

$$-\frac{p_{\mathrm{re}}(\varphi)}{p_{\mathrm{re}}(\varphi)^2+p_{\mathrm{im}}(\varphi)^2}+\frac{1}{\gamma_3}\cos(\theta)$$
$$\frac{p_{\mathrm{im}}(\varphi)}{p_{\mathrm{re}}(\varphi)^2+p_{\mathrm{im}}(\varphi)^2}+\frac{1}{\gamma_3}\sin(\theta) \quad (29)$$

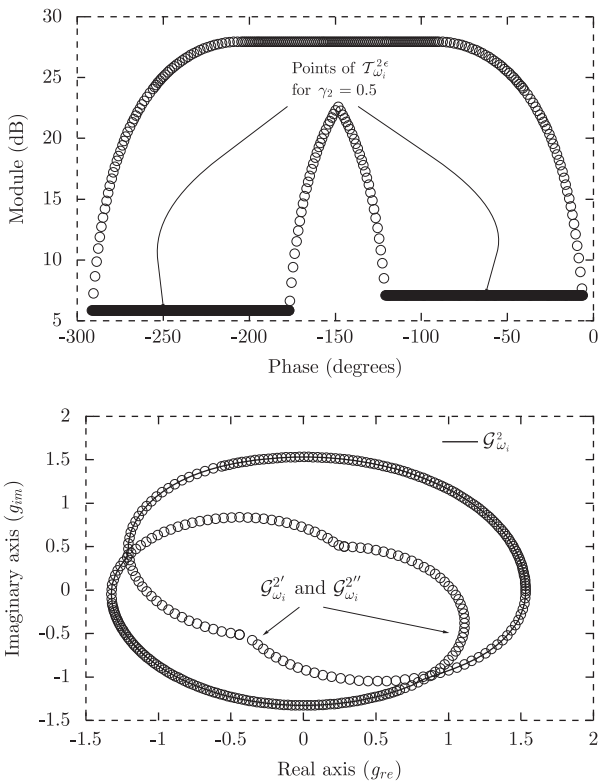

Figure 8. $\mathscr{T}^{2\varepsilon}_{\omega_i}$ compound of two pieces (above) and the final controller bound (below).

[‡‡]Extreme circumferences are defined for $\varphi=\varphi_1$ and $\varphi=\varphi_2$.

[§§]A controller bound defines an area of the Re–Im plane where the controller can be located. The intersection of the areas of different controller bounds gives the most unfavorable case.

DOI: 10.1002/rnc

In this case, the radius is constant, $r(\varphi)=1/\gamma_3$. Therefore, inequality (16) is not fulfilled and (14) can be applied. See [27] for an example of the envelope method in this case.

6. ROBUST CONTROL EFFORT BOUND

The control specification for control effort is $|G/(1+\mathscr{P}G)|\leqslant\gamma_4$. In this case, let us substitute in (1) $A(\mathrm{j}\omega)=0$, $B(\mathrm{j}\omega)=1$ and $C=\mathscr{T}_{\omega i}(\varphi)=p_{\mathrm{re}}(\varphi)+\mathrm{j}p_{\mathrm{im}}(\varphi)$. The inequality (3) becomes

$$(g_{\mathrm{re}}^2+g_{\mathrm{im}}^2)(\gamma_4^2(p_{\mathrm{re}}^2+p_{\mathrm{im}}^2)-1)+2\gamma_4^2 g_{\mathrm{re}}p_{\mathrm{re}} -2\gamma_4^2 g_{\mathrm{im}}p_{\mathrm{im}}+\gamma_4^2\geqslant 0 \tag{30}$$

When this expression is equal to zero, the family of circumferences is:

$$\begin{aligned}&\frac{-\gamma_4^2 p_{\mathrm{re}}(\varphi)}{\gamma_4^2(p_{\mathrm{re}}(\varphi)^2+p_{\mathrm{im}}(\varphi)^2)-1}\\ &\quad+\frac{\gamma_4}{\gamma_4^2(p_{\mathrm{re}}(\varphi)^2+p_{\mathrm{im}}(\varphi)^2)-1}\cos(\theta)\\ &\frac{\gamma_4^2 p_{\mathrm{im}}(\varphi)}{\gamma_4^2(p_{\mathrm{re}}(\varphi)^2+p_{\mathrm{im}}(\varphi)^2)-1}\\ &\quad+\frac{\gamma_4}{\gamma_4^2(p_{\mathrm{re}}(\varphi)^2+p_{\mathrm{im}}(\varphi)^2)-1}\sin(\theta)\end{aligned} \tag{31}$$

The radius is only a function of the module because $r=\gamma_4/(\gamma_4^2 m^2-1)$ where $m=\sqrt{p_{\mathrm{re}}(\varphi)^2+p_{\mathrm{im}}(\varphi)^2}$. Then, its largest variation appears when $\mathscr{T}_{\omega_i}(\varphi)$ is built from an uncertain gain, see (20). Expression (16) becomes:

$$\frac{(m_1^2+m_2^2)\gamma_4^4}{((m_1^2+m_2^2)\varphi^2\gamma_4^2-1)^2}<0 \tag{32}$$

that is impossible to achieve. Therefore, each pair of two infinitesimally close circumferences has always at least one common point.

Despite (16) or (32) are not met, it cannot be concluded that every point in the template contour

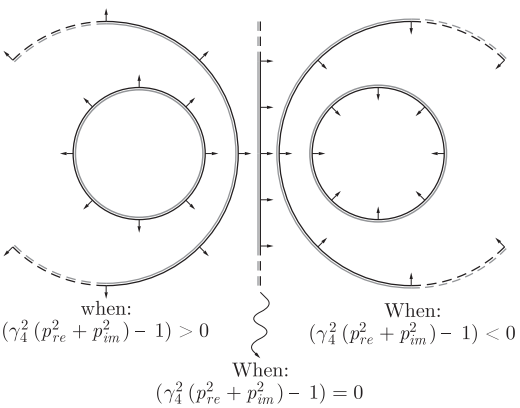

Figure 9. Circumference evolution from positive to negative $\gamma_4^2(p_{\mathrm{re}}(\varphi)^2+p_{\mathrm{im}}(\varphi)^2)-1$ values.

$\mathscr{T}_{\omega_i}(\varphi)$ generates a controller bound point and further analysis is necessary. Some template contour points could achieve both $\gamma_4^2(p_{\mathrm{re}}(\varphi)^2+p_{\mathrm{im}}(\varphi)^2)-1>0$ or $\gamma_4^2(p_{\mathrm{re}}(\varphi)^2+p_{\mathrm{im}}(\varphi)^2)-1<0$. The sign variation in this expression produces a high variation of the circumference center $(g_{\mathrm{rc}}(\varphi), g_{\mathrm{ic}}(\varphi))$ and the radius $r(\varphi)$ sign. A positive radius implies that the outer envelope curve keeps inequality (30). A negative radius implies that (30) is kept by the inner envelope curve. If $\gamma_4^2(p_{\mathrm{re}}(\varphi)^2+p_{\mathrm{im}}(\varphi)^2)-1=0$, the circumference becomes a line. Taking this into account, the template contour points such that $\gamma_4^2(p_{\mathrm{re}}(\varphi)^2+p_{\mathrm{im}}(\varphi)^2)-1<0$ will give the less favorable bound. Figure 9 shows the evolution of the circumference family when the sign of the earlier expression changes from positive to negative. Circumferences are bi-coloured (black and gray) to identify each side of the plane they divide and the arrows indicate the part of the plane that keeps the control specification.

The following can be concluded: for those templates where every point keeps $\gamma_4^2(p_{\mathrm{re}}(\varphi)^2+p_{\mathrm{im}}(\varphi)^2)-1>0$, the controller bound is determined by the outer envelope curve of the family. For templates where every point keeps $\gamma_4^2(p_{\mathrm{re}}(\varphi)^2+p_{\mathrm{im}}(\varphi)^2)-1<0$, the controller bound is determined by the inner envelope curve of the family. For templates where some points keep $\gamma_4^2(p_{\mathrm{re}}(\varphi)^2+p_{\mathrm{im}}(\varphi)^2)-1>0$ and others keep $\gamma_4^2(p_{\mathrm{re}}(\varphi)^2+p_{\mathrm{im}}(\varphi)^2)-1<0$, the controller bound is

DOI: 10.1002/rnc

only determined by the template points that keep the last inequality (those that produce negative radius).

7. REMARKS

The envelope method allows the designer to calculate analytical QFT bounds for robust performance and robust stability control specifications with the following advantages:

- The new algorithm avoids the computational nested loops for the discrete value set of the controller's phase used in Borghesani's [19] toolbox or the discrete value set of the nominal open loop in the cross section method [20, 22, 23], as well as the nested loops for the discrete value set of the plant required in all those methods. Hence, accuracy is improved and computational effort is significantly reduced.
- There is no restriction to compute multivalued bounds. Then, it is possible to calculate all the points that define the QFT bound at each phase.
- The solution bound is expressed as an analytical function on the independent variable φ, used to track the plant template contour. Thus, the mathematical results are based on the use of $\mathcal{T}_{\omega_i}(\varphi)$. This function of a variable φ can be obtained by approximating the discrete contour of the ω_i-template. In [7, 8] it is shown how this discrete contour is approximated using the Fourier series.
- The use of analytical functions for the bound expressions, apart from improving accuracy and reducing computational cost, gives the definition of algebraical and geometrical properties and finds a relationship between the template points (equivalent template $\mathcal{T}^{\varepsilon}_{\omega_i}$) and the bound points.
- To use the envelope method, the derivative of the template contour $\mathcal{T}_{\omega_i}$ must exist. Then, it is necessary to make the corners of $\mathcal{T}_{\omega_i}$ round. This is a simple task and produces a negligible error. One solution to make round a discrete template contour defined by the array `p` of consecutive points could be:

```
k=2; angmin=5.5*pi/6;
while k<length(p),
    %Angle between two consecutive lines:
     angulo=abs(angle(p(k-1)-p(k))-angle(p(k+1)-p(k)));
    if angulo>pi, angulo=2*pi-angulo;end
  if angulo<angmin,
     p(k)=(p(k-1)+p(k)+p(k+1))/3;
     k=k-2;
  end
  k=k+1;
end
```

- The reference tracking specification is formulated by using the form: $\gamma_{5\,\mathrm{inf}} < |FPG/(1+PG)| < \gamma_{5\,\mathrm{sup}}$, which needs a 2 DoF (prefilter and controller) control structure. When this double inequality is reduced to one of the form (1), two uncertain transfer functions and two template contours arise, instead of just one as the envelope method formulates. New research is needed for this case, being it out of the scope of this paper.

8. EXAMPLES

This section shows two examples of QFT bounds computation using the envelope method. In the first subsection, a case of robust sensitive reduction is studied. The second subsection shows how the method works calculating control effort bounds. The envelope method is compared with the Borghesani toolbox method [19] in both cases. Additional examples of robust stability and robust disturbance rejection at plant input bounds can be found in [27].

DOI: 10.1002/rnc

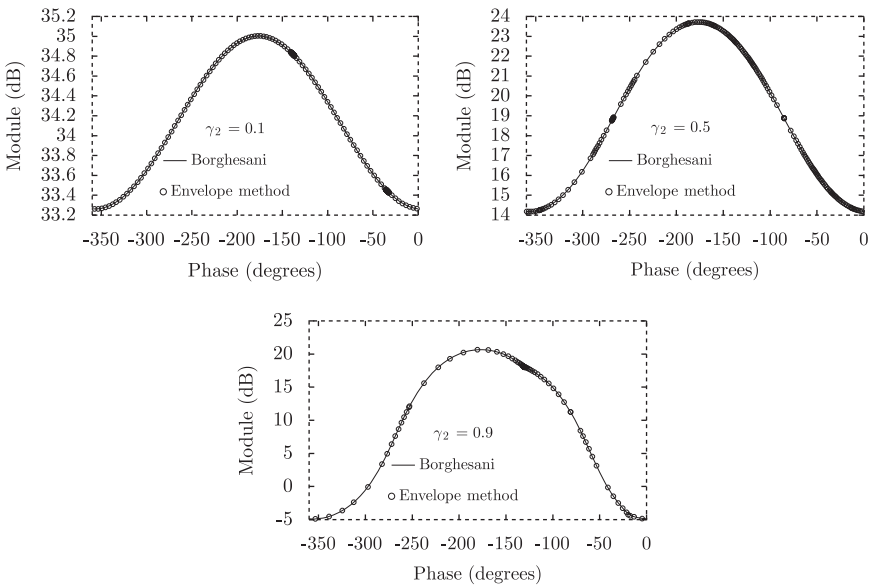

Figure 10. Bounds for the specifications of the example.

8.1. Example 1: Robust disturbance rejection at the plant output

Let us consider the plant:

$$\mathscr{P}(s)=\frac{k\mathrm{e}^{-0.3s}}{(s+a)(s+20)},\quad k\in[1,10],\quad a\in[1,5] \qquad (33)$$

The aim is to obtain the bounds for robust disturbance rejection at the plant output at $\omega=5\,\mathrm{rad/s}$: $|1/(1+\mathscr{P}G)|<\gamma_2$, for the specifications $\gamma_2=0.1$, 0.5 and 0.9.

First, the discrete template is computed with an adequate number of points (in this case a 400 element array). Then, g_{rc}, g_{ic} and r are obtained using (24). After that, their derivatives are calculated. The examples presented in this paper use the forward difference method to compute the derivatives, that is

$$f'(x_1)=\frac{f(x_1+\varepsilon)-f(x_1)}{\varepsilon}$$

Note that the truncation error is of εth order although its exact computation is unfeasible because the function $\mathscr{T}_{\omega_i}$ is unknown. The derivative is obtained from the 400 element array that defines the discrete contour template, performing the difference between the $n+1$ and the n elements of this array. If the points defined in $\mathscr{T}_{\omega_i}$ are close enough, this approximation works fine as it is shown in the comparative results.

Previously, the equivalent template for each specification value must be calculated. Finally, the bounds can be obtained by substituting the θ parameter of (24) with (14). Figure 10 shows them.

The results obtained with Borghesani's toolbox are bounds defined by an equidistant phases set (73 phases by default). The number of points obtained using the envelope method is equal to the number of points of the discrete template contour (although $\mathscr{T}_{\omega_i}(\varphi)$ is an analytical function, it must be discretized to be used with a computational program). Therefore, the number of points obtained with the envelope method is usually quite higher than the one obtained with the Borghesani's toolbox (because the number of template points can be several hundreds).

The computation time required by the Borghesani toolbox was 265 ms for the three bounds. The envelope method took 11 ms. The commands *tic-toc* were used running on Windows XP and Matlab QFT toolbox [19] over a PC with a 1.4 GHz Pentium IV processor and 512 Mb RAM.

DOI: 10.1002/rnc

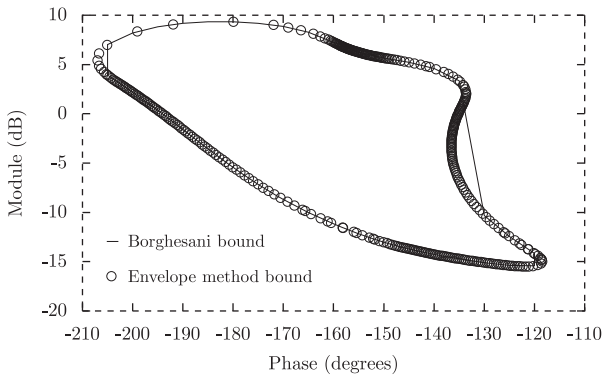

Figure 11. Control effort bound computed using the Borghesani toolbox and the envelope method.

8.2. *Example 2: Robust control effort bound*

It is desired to compute the robust control effort bound at $\omega = 5\,\text{rad/s}$ for the plant:

$$\mathscr{P} = \frac{500\text{e}^{-0.3s}}{(s+a)(s+6b)} \tag{34}$$

where $a \in [1, 5]$ and $b \in [1, 10]$. The control effort specification at $\omega = 5\,\text{rad/s}$ is $|G/(1+\mathscr{P}G)| < 2$.

In a similar way as the one indicated in the previous example, the values of g_{rc}, g_{ic}, r and their derivatives are computed. Using (31) the bound is obtained. Figure 11 shows the results comparing different methodologies.

The computation time required with the envelope method was twenty times lower than the one required with the Borghesani method. Besides, this example shows that the envelope method is able to compute multivalued bounds. Note that accuracy was also greater with the envelope method because there was not loss of bound extreme points.

9. CONCLUSIONS

This paper has described a new analytical formulation to compute QFT bounds based on envelope curves. The controller bound has been defined by the envelope curve of a family of circumferences as an analytical function with some useful properties. In comparison with other methods, computational effort does not increase geometrically with the number of discrete template points and discrete bound phase points since: (a) the bound phase is not discretized; (b) computational nested loops are not used to track both discrete template and phase sets (gridding methods). The significant reduction of computational effort allows the user to deal with a large number of template points, and therefore improves accuracy. The method also allows the designer to calculate multivalued bounds. The advantages have been illustrated with two examples: robust disturbance rejection at the plant output and robust control effort.

REFERENCES

1. Horowitz IM. *Synthesis of Feedback Systems*. Academic Press: New York, 1963.
2. Horowitz IM, Sidi M. Synthesis of feedback systems with large plant ignorance for prescribed time-domain tolerances. *International Journal of Control* 1972; **16**:287–309.
3. Horowitz IM. Survey of quantitative feedback theory (QFT). *International Journal of Control* 1991; **53**(2):255–291.
4. Houpis CH, Rasmussen SJ, García-Sanz M. *Quantitative Feedback Theory*, *Fundamentals and Applications* (2nd edn). Taylor & Francis: FL, U.S.A., 2006.
5. Yaniv O. *Quantitative Feedback Design of Linear and Non-linear Control Systems*. Kluwer Academic Publishers: Dordrecht, MA, U.S.A., 1999.
6. Horowitz IM. Some ideas for QFT research. *Fifth International Symposium on Quantitative Feedback Theory and Robust Frequency Domain Methods*, Pamplona (Spain), July 2001; 57–61.
7. Martín-Romero JJ, Martín-Romero A. QFT templates for plants with a high number of uncertainty parameters. *IEEE Transactions on Automatic Control* 2007; **52**(4):754–758.
8. Martín-Romero JJ, Gil-Martínez M, García-Sanz M. Analytical formulation to compute QFT templates for plants with a high number of uncertainty parameters. *Mediterranean Conference on Control and Automation*, Athens, Greece, June 2007.
9. Longdon L, East DJ. A simple geometrical technique for determining loop frequency bounds which achieve prescribed sensitivity specifications. *International Journal of Control* 1978; **30**(1):153–158.
10. Houpis CH, Lamont GB. *ICECAP-QFT Users Manual*. Electrical and Computer Department, Air Force Institute of Technology, Wright-Paterson AFB, 1988.
11. Thompson DF, Nwokah ODI. Stability and optimal design in quantitative feedback theory. *Proceedings of the ASME Winter Annual Meeting Conference*, San Francisco, U.S.A., ASME Paper No. 89-WA/DSC-39, 1989.

DOI: 10.1002/rnc

12. Bailey FN, Hul CH. CACSD tools for loop gain-phase shaping design of SISO robust controllers. *Proceedings of the IEEE Control System Society Workshop on Computer Aided Control System*, Tampa, FL, U.S.A., 1989; 151–157.
13. Wang GG, Chen CW, Wang SH. Equations for loop bound in quantitative feedback theory. *Proceedings of the 30th Conference on Decision and Control*, Brighton, U.K., 1991; 2968–2969.
14. Chait Y, Yaniv O. Multi-input/single-output computer-aided control design using the quantitative feedback theory. *International Journal of Robust and Nonlinear Control* 1993; **3**:47–54.
15. Yaniv O, Chait Y. Direct robust control of uncertain sampled-data systems using the quantitative feedback theory. *Proceedings of the American Control Conference*, Boston, U.S.A., 1991.
16. Yaniv O, Chait Y. A simplified multi input/output formulation for the quantitative feedback theory. *Journal of Dynamic Systems*, *Measurements and Control* 1992; **114**: 179–185.
17. Yaniv O, Chait Y. Direct control design in sampled-data uncertain systems. *Automatica* 1993; **29**(2):365–372.
18. Chait Y, Borghesani C, Yaniv O. Single-loop QFT design for robust performance in the presence of non-parametric uncertainties. *ASME Journal of Dynamic Systems*, *Measurement*, *and Control* 1995; **117**:420–424.
19. Borghesani C, Chait Y, Yaniv O. *Quantitative Feedback Theory Toolbox User's Guide*. The MathWorks Inc: U.S.A.
20. Gutman P-O. The toolbox for robust control systems design for use with Matlab, *User's Guide and Reference Guide*. Manuals downloadable from http://www.math.kth.se/optsyst/research/5B5782/index.html, 1996.
21. Bailey FN, Panzer D, Gu G. Two algorithms for frequency domain design of robust control systems. *International Journal of Control* 1988; **48**(5):1787–1806.
22. Moreno JC, Baños A, Berenguel M. Improvements on the computation of boundaries in QFT. *International Journal of Robust and Nonlinear Control* 2006; **16**:575–597.
23. Gutman P-O, Nordin M, Cohen B. Recursive grid methods to compute value sets and Horowitz–Sidi bounds. *International Journal of Robust and Nonlinear Control* 2006; **17**: 155–171.
24. Zhao Y, Jayasuriya S. On the generation of QFT bounds for general interval plants. *ASME Journal of Dynamic Systems*, *Measurements and Control* 1994; **116**:618–627.
25. Rodrigues JM, Chait Y, Hollot CV. An efficient algorithm for computing QFT bounds. *ASME Journal of Dynamic Systems*, *Measurements and Control* 1997; **119**(3):548–552.
26. Nataraj PSV, Sardar G. Computation of QFT bounds for robust sensitivity and gain-phase margin specifications. *ASME Journal of Dynamic Systems*, *Measurements and Control* 2000; **122**:528–534.
27. Martín-Romero JJ, Gil-Martínez M, García-Sanz M. Analytical formulation of robust performance/stability bounds for QFT controller design. *European Control Conference*, Kos, Greece, July 2007.
28. Martín-Romero JJ, Gil-Martínez M, García-Sanz M. The envelope method to compute analytical QFT bounds. *Eighth International Symposium on Quantitative Feedback Theory and Robust Frequency Domain Methods*, Rehovot, Israel, July 2007.
29. Boltianski VG. *La envolvente* Editorial MIR Moscú, 1977.
30. García-Sanz M, Vital P. Efficient Computation of the frequency representation of uncertain systems. *Fourth International Symposium on Quantitative Feedback Theory and Robust Frequency Domain Methods*, Durban, South Africa, 1999; 117–126.
31. Boje E. Finding nonconvex hulls of QFT templates. *ASME Journal of Dynamic Systems*, *Measurements and Control* 2000; **122**(1):230–232.

DOI: 10.1002/rnc